Kokai Tokkyo Koho JP. 58216190 (1983) [CA **100**, 156646j(1984)].
3. S. C. Shin, H. C. Wang, W. Y. Lee, and Y. Y. Lee, *Bull. Korean Chem. Soc.*, **6**, 323 (1985).
4. S. C. Shin and Y. Y. Lee, *J. Korean Chem. Soc.*, **27**, 382 (1983).
5. S. C. Shin and Y. Y. Lee, *Bull. Korean Chem. Soc.*, **9**, 359 (1988).

Syntheses and Properties of the High-Tc Superconductive $Bi_{2-x}Mo_xSr_2Ca_2Cu_3O_y$ System

Keu Hong Kim*, Jong Tae Lim, Seung Koo Cho, Byoung Chan Kwak, Don Kim†, and Jae Shi Choi

Department of Chemistry, Yonsei University, Seoul 120-749. *Received September 11, 1989*

The superconducting properties have been studied for high-Tc superconductors of the $Bi_{2-x}Mo_xSr_2Ca_2Cu_3O_y$ system (x = 0.03-0.30). The crystal structure is pseudo tetragonal with the average lattice parameters a = 5.38 Å, b = 5.44 Å and c = 30.6 Å. All samples exhibit superconductivity with Tc offset at 79 K and Tc onset at 90-115 K. The Tc onset point decreases with increasing x, but the Tc offset points are nearly the same for all samples. Scanning electron micrographs show a special growth behavior of the grains with a plate shape. It is suggested that the decrease in Tc onset points with substitution of Mo for Bi is due to the decrease in lattice parameters and to the p-orbital of Mo. It is concluded that Mo does not play a crucial role in the superconducting transition of the $Bi_2Sr_2Ca_2Cu_3O_y$ system.

Introduction

Maeda *et al.*[1] were the first to synthesize a superconducting composition of $BiSrCaCu_2O_x$ (1112) which had a Tc of about 105 K, but with a low-temperature tail extending to 80 K. They reported that the composition must contain both Sr and Ca in order to have a high-Tc phase. The $Bi_2Sr_2Ca_2Cu_3O_y$ (2223) phase[2] has been synthesized by D. Kim *et al.*[3] and it exhibits superconductivity with Tc onset at 120 K and Tc offset at 79 K. They report that the 2223 composition can easily contain a low-Tc phase depending on thermal treatment condition.

Recently, K. H. Kim *et al.*[4] have synthesized 1111, 1112 and 1113 compositions and studied their Raman spectra. They have found that the Raman line at 630 cm^{-1} is the most intense, corresponds to the (zz) configuration and is assigned to Cu-O stretching vibration along the c axis. However, this strong band at 630 cm^{-1} is split into at least two components, 629 and 655 cm^{-1}, indicating the presence of distinct Cu-O bonds along the c axis, especially for the samples with a low-Tc phase.

To study a possible structure ordering effect in the Bi-Sr-Ca-Cu-O system with a low-Tc phase, high-Tc superconducting materials, $(Bi_{1-x}Pb_x)_4Sr_3Ca_3Cu_4O_{16-\delta}$ with a variable amount of Pb (x = 0.1-0.5) have been synthesized and studied by electron microprobe analysis, x-ray diffraction, resistivity measurement and micro-Raman spectroscopy[5]. They have found that the optimum effective Pb amount for the best high-Tc superconductivity, with a single phase (high-Tc phase), is around 12 percent. They have also observed that the intensity of the 655 cm^{-1} (Cu-O stretching vibration) line decreases with increasing Pb content, and finally disappears at x = 0.5, where the intensity of the 630 cm^{-1} line is maximum. Based on the Raman data, they have suggested that the Cu-O bond in $(Bi_{1-x}Pb_x)_4Sr_3Ca_3Cu_4O_{16-\delta}$ becomes more homogeneous, a low-Tc phase disappears, and onset Tc increases due to the substitution of Pb for Bi.

In this study, Mo has been substituted for Bi in the superconducting 2223 phase with a variable amount of Mo at a nominal Mo mol percent of x = 0.03-0.30 to see if Mo eliminates the low-Tc phase, enhances onset Tc and increases homogeneity of the Cu-O bond as Pb does in the Bi-Sr-Ca-Cu-O system.

Experimental

Sample Preparation and Analysis. A number of compositions in the $Bi_{2-x}Mo_xSr_2Ca_2Cu_3O_y$ system were prepared from a mixture of Bi_2O_3, MoO_3, $SrCO_3$, $CaCO_3$ and CuO powders (each 99.9% pure). The starting powder materials were ball mill mixed and calcined at 750 °C in air for 12 h. The well-mixed powder was pressed into a pellet at a pressure of 49 MPa. The pellet was then heated at 840 °C in air for three days and quenched to room temperature.

Inductive coupled plasma (ICP) analysis was performed to determine effective Mo mol percent in the sample. Differential thermal analysis (DTA) and thermogravimetric analysis (TGA) were performed to check the change in defect concentration and phase transition and to determine the calcination and sintering temperatures. X-ray diffraction (XRD) was carried out to detect crystal structure and formation of solid solution, on a diffractometer (Philips 1710, CuKα) equipped with a curved graphite monochrometer in the scattered beam path. Scanning electron microprobe (SEM) analysis was also

†Present address: General Education Department, Pusan National Institute of Technology, Yongdang-dong 100, Nam-gu, Pusan 608-080

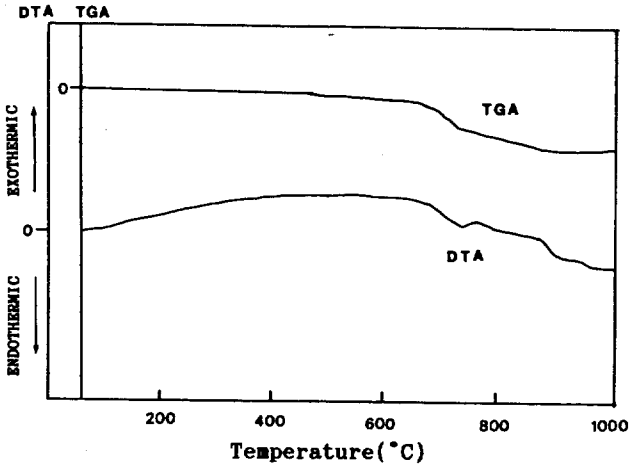

Figure 1. DTA and TGA curves of unsintered $Bi_2Sr_2Ca_2Cu_3O_y$.

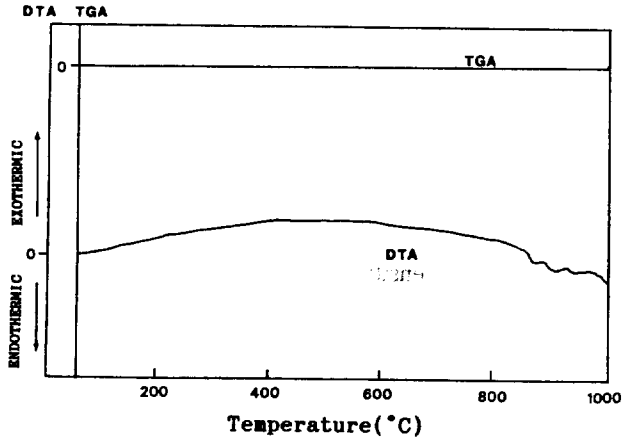

Figure 2. DTA and TGA curves of sintered $Bi_2Sr_2Ca_2Cu_3O_y$.

performed to compare the morphology of the sample.

Resistivity Measurement. A specimen about 1 mm × 1.5 mm × 5 mm in size was cut from the pellet for resistance measurement by a standard four-probe *ac* technique. Copper wires were used as electrical leads and attached to the sample with indium. The current used to measure the electrical resistance was 1/600–0.5/600 A, and the resolution of the voltage measurement was 100 μV. The resistance and transition temperature were not affected by the current in this range. The frequency was 110 Hz. The potential difference was measured with a lock-in amplifier (EG & G Co. PARC 5210) up to 100 μV on an IBM-PC/AT. The temperature was measured with a copper-constantan thermocouple. A compensation board (PCLD 789 MUX) and a 14-bit A/D converter (PCL 714) were used to calculate voltage into temperature, and the error range of temperature was ±0.01 °C.

Results and Discussion

Figures 1 and 2 show the DTA and TGA curves of unsintered and sintered $Bi_2Sr_2Ca_2Cu_3O_y$ systems, respectively. As shown in Figure 1, the unsintered mixture begins to react at around 650 °C and a heat absorption peak due to melting appears around 850 °C. Comparing the TGA curve at room temperature with that at 850 °C, about 13% loss of mass is

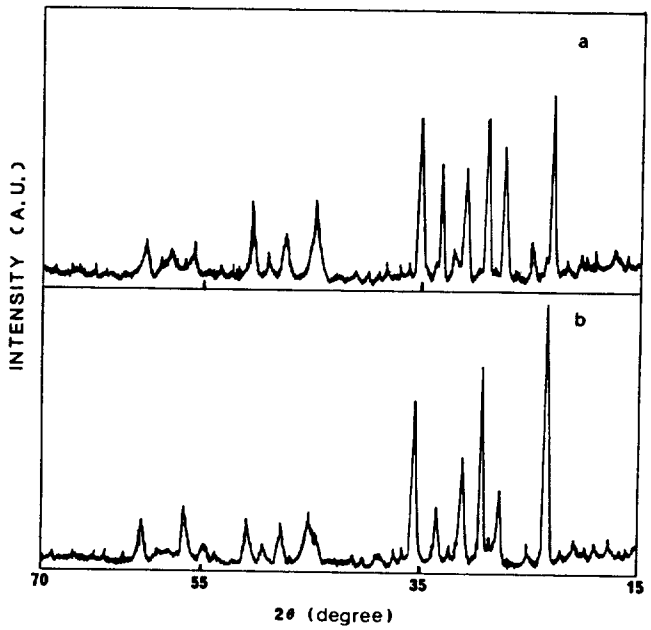

Figure 3. Typical x-ray diffraction patterns of $Bi_{1.97}Mo_{0.03}Sr_2Ca_2Cu_3O_y$(a) and $Bi_{1.70}Mo_{0.30}Sr_2Ca_2Cu_3O_y$(b), respectively.

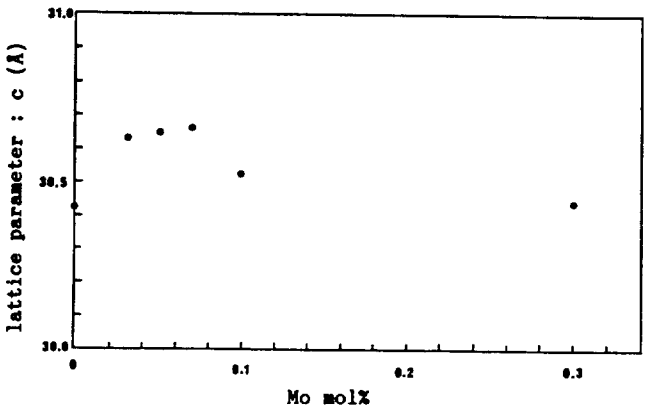

Figure 4. Lattice parameter(c) *vs.* Mo mol %.

observed. This is due to CO_2(g) decomposition from $SrCO_3$ and $CaCO_3$ in the mixture. The value of 13% is different from the theoretical value of 14.8%; the difference of 1.8% may come from undecomposed materials. Based on the DTA and TGA data in Figure 1, the mixture was sintered at 840 °C for 3 days to decompose carbonates completely. As can be seen in Figure 2, no loss of mass and no phase transition occur and a heat absorption peak appears at 850–950 °C.

Figure 3 shows typical X-ray diffraction patterns of $Bi_{1.97}Mo_{0.03}Sr_2Ca_2Cu_3O_y$ (a) and $Bi_{1.70}Mo_{0.30}Sr_2Ca_2Cu_3O_y$ (b), respectively. As shown in Figure 3, the positions of peaks shift to higher angles (2θ) as the amount of Mo increases, indicating a decrease in d value. From indexation of the X-ray diffraction spectrum for each sample, the lattice parameters were obtained.

Figure 4 shows the lattice parameter(c) *vs* Mo mol%. The lattice parameter increases with increasing Mo mol% up to $x = 0.07$ and then decreases with $x = 0.1$ and $x = 0.3$. The increasing lattice parameter implies that substitution of Mo for Bi is very difficult up to 0.07 Mo mol% and the Mo ion is

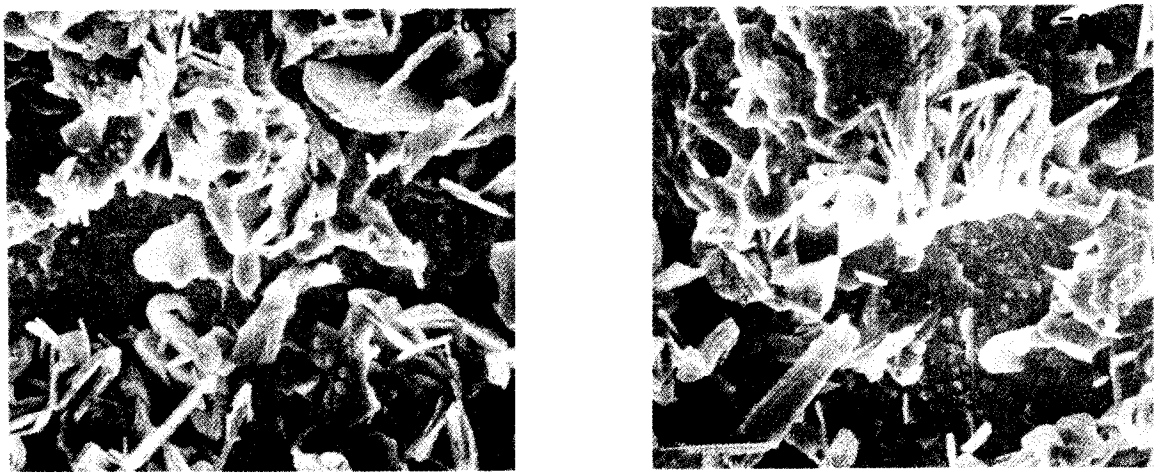

Figure 5. SEM photographs of the $Bi_{2-x}Mo_xSr_2Ca_2Cu_3O_y$ system with $x = 0.00$ and 0.03, respectively.

Figure 6. SEM photographs of the $Bi_{2-x}Mo_xSr_2Ca_2Cu_3O_y$ system with $x = 0.07$, 0.10 and 0.30, respectively.

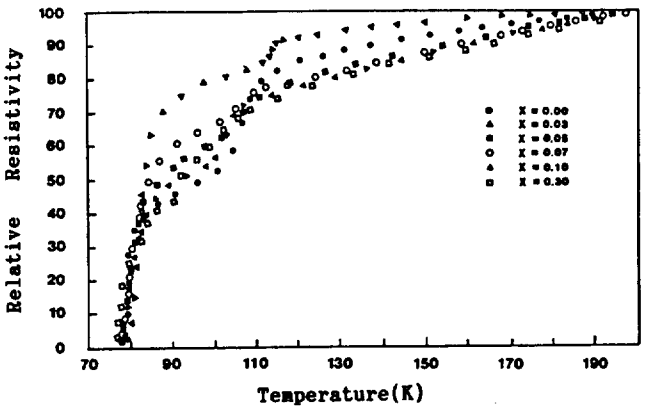

Figure 7. Temperature dependency of the resistivity of $Bi_{2-x}Mo_xSr_2Ca_2Cu_3O_y$ as a function of Mo mol %.

sited at an interstitial position rather than a Bi ion position. On the other hand, the lattice parameter for 0.1 or 0.3 Mo mol% indicates that partial substitution of Mo for Bi is possible in this system.

Figures 5 and 6 show the SEM photographs of the $Bi_{2-x}Mo_xSr_2Ca_2Cu_3O_y$ system with $x = 0.00$, 0.03, 0.07, 0.10 and 0.30. As can be seen in these figures, the samples with $x = 0.03$ and 0.07 have many particles of needle shape, but the samples with $x = 0.10$ and 0.30 have a flat form.

Figure 7 shows the temperature dependency of the resistivity as a function of Mo mol%. As shown in Figure 7, the samples with Mo mol% up to 7 have onset Tc at 115 K, but the samples with $x = 0.10$ and $x = 0.30$ have onset Tc at 100 and 90 K, respectively. The zero resistivity is 79 K for all samples. The onset Tc decreases with increasing Mo mol%. Based on the resistivity data, the $Bi_{2-x}Mo_xSr_2Cu_3O_y$ superconductors with $x = 0.07$–0.30 have two phases, designated the low- and high-Tc phases.

From the lattice parameter (Figure 4) and the resistivity (Figure 7), it is suggested that the substitution of Mo for Bi decreases the onset Tc, possibly because the *p*-orbital of Mo^{6+} blocks the current pathway of the tubular molecular orbital due to the $O(p\pi)$–$O(p\pi)$ hole from the Cu–O plane.

Acknowledgement. The financial support of the Ministry of Science and Technology is gratefully acknowledged. The authors are grateful to Professor Robert G. Sauer, Department of Physics, for helpful discussion.

References

1. H. Maeda, Y. Tanaka, M. Fukutomi and T. Asano, *Jpn. J. Appl. Phys. Lett.*, **4**, L209 (1988).
2. J. M. Tarascon, W. R. McKinnon, P. Barboux, D. M. Hwang, B. G. Bagley, L. H. Greene, G. W. Hull, Y. LePage, N. Stoffel and M. Giround, *Phys. Rev. B*, **38**, 8885

(1988).
3. D. Kim, S. K. Cho, J. T. Lim, K. H. Kim and J. S. Choi, *J. Kor. Chem. Soc.*, **32**, 603 (1988).
4. P. V. Huong, E. Oh-Kim, K. H. Kim, D. Kim and J. S. Choi, *Mater. Sci. Eng.*, **A109**, 337 (1989).
5. K. H. Kim, P. V. Huong, E. Oh-Kim, M. Lalhaye, S. K. Cho and B. C. Kwak, Private Communication (1989).

Viscosity of Liquids under High Pressures

Wonsoo Kim*, Hyungsuk Pak†, and Tong-Seek Chair‡

Department of Metallurgy, Hong Ik Technical College, Seoul 121-791
†Department of Chemistry, Seoul National University, Seoul 151-742
‡Department of Chemistry, Korea University, Seoul 136-701. *Received October 5, 1989*

By using Pak's theory of liquid, a phenomenological theory of viscosity proposed by the authors is applied to liquids under high pressures. The calculated viscosities for various simple substances are in good agreements with those of the observed values over wide pressure ranges.

Introduction

Research on transport properties at high pressures has developed vigorously in recent 30 years. The general behavior of these properties in the gaseous phase is well understood, and it has become possible, to some extent, to interpret theoretically and to predict empirically the effect of high pressure. On the other hand, the transport properties of liquids under pressure have not always been interpreted both empirically and theoretically[1].

For the viscosity of liquids, some theories[2-4] accurately describe the temperature dependence, but these theories fail to account for the variation of the viscosities with pressure. Only one idea assumed by these theories is that the solid volume V_s decreases with increasing pressure. The purpose of this paper is to show that our viscosity equation[5] adequately describes the effect of pressure on the viscosities of liquids.

Theory

Our equation for the viscosity of fluids has the simple form

$$\eta = \tau P_a \tag{1}$$

where τ and P_a are the collision time and absolute pressure (kinetic pressure + internal pressure), respectively. The collision time and the absolute pressure of the fluid are related to the thermodynamic properties of the system as follows

$$\tau = (\pi d^2 n_{ph})^{-1} (\gamma/\rho\beta_T)^{-\frac{1}{2}} \tag{2}$$

$$P_a = 2T\frac{\alpha_P}{\beta_T} - P \tag{3}$$

where d is the collision diameter, n_{ph} is the phonon number density, γ is the heat capacity ratio, and ρ is the fluid density.

β_T is he isothermal compressibility, α_P is the isobaric thermal expansion coefficient and P is the pressure. For the calculation of the viscosity at high pressure, we have to know the thermodynamic properties such as ρ, p, α_P, β_T and γ. But unfortunately the experimental value of such properties of liquids have not been known widely at high pressures. Therefore, we can calculate this thermodynamic properties at high pressure using the state equation of the liquid.

According to Pak's theory[6], the partition function of the liquid Q is given as follows

$$Q = \frac{N_t!}{N_s!\,(N_t - N_s)!}\left[\frac{e^{E_s/RT}}{(1-e^{-\theta/T})^3}\right]^{N_s} \left[\frac{(2\pi mkT)^{3/2}(V-V_s)}{h^3}\right]^{N_g}\frac{1}{N_g!} \tag{4}$$

where E_s, V_s and E_g are the ground state energy and the molar volume of the solid like molecule and the potential energy of the gas like molecule, respectively. θ is the Einstein characteristic temperature and N_t, N_s and N_g are $N(\frac{V}{V_s})$, $N(\frac{V_s}{V})$ and $N(\frac{V-V_s}{V})$ respectively; here N is the Avogdro number. The parametric values E_s, θ, E_g and V_s can be found by the use the following equations

$$P = -\left(\frac{\partial A}{\partial V}\right)_{T,N} \tag{5}$$

$$S = -\left(\frac{\partial A}{\partial T}\right)_{V,N} \tag{6}$$

$$A + pV = A_g + pV_g \tag{7}$$

where A_g and V_g are the Helmholtz free energy and the